Journal of Mines, Metals and Fuels, *71(8) : 1074-1080; 2023. DOI: 10.18311/jmmf/2023/35232*

Print ISSN : 0022-2755

Journal of Mines, Metals and Fuels

Contents available at: *www.informaticsjournals.com/index.php/jmmf*

A Study on Structural, Electrical and Ethanol Sensing Properties of RGO Substituted SnO_2 Nanoparticles

H. V. Kiranakumar[1,2], C. S. Naveen[1,2]*, R. Thejas[1,2,] G. D. Prasanna[3], G. Nagaraju[4], K. Swaroop[5] and M. V. Murugendrappa[6]

[1]Department of Physics, School of Engineering, Presidency University, Bengaluru – 560064, Karnataka, India
[2]Materials Research Center, Presidency University, Bengaluru – 560064, Karnataka, India; naveen@presidencyuniversity.in
[3]Department of Studies in Physics, Davangere University, Davangere – 577007, Karnataka, India
[4]Energy Research Laboratory, Department of Chemistry, Siddaganga Institute of Technology, Tumakuru – 572103, Karnataka, India
[5]Department of Physics, G M Institute of Technology, Davangere – 577006, Karnataka, India
[6]Department of Physics, BMS College of Engineering, Bengaluru – 560019, Karnataka, India

Abstract

In this work RGO-SnO_2 (RGS) nanocomposites were synthesized by ex-situ polymerization method by varying the concentrations of RGO nanoparticles in SnO_2 matrix (0, 5, 10, 15, 20 wt%). The synthesized nanocomposites were subjected to structural characterizations viz, X-Ray Diffraction (XRD), Fourier Transform Infrared Spectroscopy (FTIR), Field Emission Scanning Electron Microscopy (FESEM) techniques. XRD and FTIR spectroscopic studies reveals the presence of characteristic bands of both RGO, SnO_2 nanoparticles and formation of their composites confirmed with the interfacial interaction of RGO nanoparticles in the SnO_2 systems. FESEM images of RGS nanocomposites depicts the spherical morphology. Electrical properties of the synthesized samples were studied with respect to the frequency range 100 Hz to 5 MHz at room temperature. The gas sensing performance of the RGS nanocomposites were studied at 3 different temperatures (200, 250, 300 ^{0}C) for 4500 PPM of ethanol vapors and at 3000C the sample 90SnO_2:10RGO shows ~145% of sensitivity with the good response of 18 s and recovery time of 194 s.

Keywords: *Ethanol Vapors, Electrical, Gas Sensing, RGO-SnO_2*

1.0 Introduction

Several gases are released, which has an effect on the environment, and this is a result of the rising population, industrialization, automobiles, air conditioners, and other sources. Studies aimed at identifying and controlling these gases are currently being conducted. The burning of fossil fuels, the emissions from automobiles (internal combustion), explosions, welding, and other human-caused causes all make major contributions as well. Novel and complex sensing methods have been developed due to the need for monitoring/controlling the ambient environment (temperature, air pressure, and humidity) in museums, organic farming, the paper industry, sophisticated instruments, pharmaceuticals, electronics manufacturing, packaging, research labs, the medical industry, and standard/calibration laboratories.

From previous research reports depicts the various forms of SnO_2 nanoparticles such as nanorods, nanotubes and nanobelts were studied, the unique structures play an important role in improving the sensing performance[1-4]. It should be noted, nevertheless, that in addition to

*Author for correspondence

structural analysis, porosity has previously been shown to be a useful method for increasing SnO_2 sensitivity to reducing gas[5].

Graphene oxide is a single-atomic-layered material that is derived from graphene, which is composed of carbon atoms arranged in a hexagonal lattice. Graphene oxide is created by the oxidation of graphene, which introduces oxygen-containing functional groups such as hydroxyl, carboxyl, and epoxy groups to the carbon lattice. This process alters the electronic and chemical properties of graphene, making it more hydrophilic and easier to process into various forms. Graphene oxide is subjected to a reduction process, which involves the removal of oxygen-containing functional groups to produce Reduced Graphene Oxide (RGO), GO is to be reduced incrementally so that the electrical conductivity can be tuned over several orders of magnitude[6,7].

Composites made of RGO-SnO_2 (RGS) materials with characteristics of both tin oxide and RGO, the semiconducting material SnO_2 has several uses, including gas detection, energy storage, etc.,[8]. A composite material including SnO_2 and RGO has greater conductivity, better gas sensing characteristics, and better electrochemical performance, when the SnO_2 nanoparticles were spread throughout the RGO matrix, the surface area is increased and the accessibility of the active sites is improved, resulting in better gas sensing characteristics[6,9]. Researchers have looked at the composites for use in various strategies, including gas sensors, lithium-ion batteries, supercapacitors, etc. RGS composites were generally synthesized in three distinct steps, (a) RGO was prepared using chemical process, (b) SnO_2 nanoparticles using a gel combustion method, (c) the prepared RGO which is then combined with SnO_2 nanoparticles using wet mixing method. Overall, RGS composites have promising properties that make them potential candidates for various applications in the various fields.

Most of the materials used so far to meet these demands belong to three categories namely semiconductors, ceramics and polymers. Only few sensors can sense ethanol at room temperature and most of them work at high operating temperatures[3]. Hence, still there is a need and scope of improving the sensor performance for ethanol vapors. One of the most crucial aspects in the field of sensors is the detection and measurement of ethanol vapor[10]. Ethanol sensors are necessary for a wide variety of industries, including the chemical, biomedical, pharmaceutical, and food industries, in particular during the production of alcoholic beverages to monitor the wine quality, clinical diagnosis, cooking, agricultural, horticultural, and veterinary analysis, contamination and pollution analysis, fermentation control and analysis, analysis of flavors and pheromones, explosives detection, and biochemical defense for the military[11]. In addition, ethanol sensors are required for the monitoring of biochemical.

In the present work, the prepared composite materials were characterized through various techniques such as X-Ray Diffraction (XRD), Fourier Transformation Infrared Spectroscopy (FTIR), Field Emission Scanning Electron Microscopy (FESEM), electrical properties were analyzed using impedance analyzer at room temperature and gas sensing studies were conducted using in-house fabricated gas sensing chamber. The sensing properties of the thick films were studied for ethanol vapors at different temperatures with 4500PPM of ethanol concentration.

2.0 Materials and Methods

2.1 Materials

All AR grade chemicals were used *viz.,* Graphite powder, Sodium nitrate, Sulphuric acid, potassium permanganate Hydrochloric acid, Hydrogen peroxide, hydrazine hydrate, tin chloride dehydrate, nitric acid, citric acid, were procured.

2.2 Sample Preparation

SnO_2 was prepared by gel combustion method, the raw materials used were tin (II) chloride dihydrate ($SnCl_2.2H_2O$) and 6.2 moles of Nitric acid (HNO_3) which is used as an oxidizer. These raw materials were dissolved in distilled water and mixed in an appropriate ratio to form a tin nitrate solution. Then Citric acid ($C_6H_8O_7$) which acts as fuel was added to this solution, the amount of citric acid was fixed at 1.5 moles. The solution was heated with constant stirring at a temperature of about 90°C in a borosilicate beaker, then the concentration of the solution slowly became higher, eventually a polymeric precursor formed, when the temperature was raised to about 300°C, the precursor underwent a strong, self-sustaining combustion reaction with evolution of large volume of gases and swelled into voluminous and foamy ashes. The

entire combustion process ended in a few minutes, the resulting ashes were then calcined at a temperature of 800^{0}C (for 2 hour) until complete decomposition of the carbonaceous residues was achieve to the obtained white powder of SnO_2 [12].

In a typical procedure, graphene oxide was synthesized from the graphite powder using a modified Hummer's method[13,14]. The typical procedure is as follows: graphite powder (2 g) and $NaNO_3$ (1 g) were combined with H_2SO_4 (46 ml) and stirred for 60 min in an ice bath. 10g of $KMnO_4$ was added to the resulting solution, and the solution was then stirred at 30 ^{0}C for 1 h. 500ml of Deionized water was added dropwise and 5ml of 30% conc H_2O_2 were slowly added to the above solution, and the resulting solution was washed with 0.1N HCl of 300 ml, additional washing with concentrated 1N HCl afforded the GO product as a powder. Subsequently, the GO powder sample was dried at 70 ^{0}C for 24 h. To generate RGO, the graphene oxide was sonicated for 2 hours at room temperature, hydrazine hydrate was added drop wise to the exfoliated graphite oxide suspension at room temperature. The reduction was performed at 100 ^{0}C for 60min, the weight ratio for hydrazine hydrate and GO was maintained at 9:7 for this sample[15]. Resultant black precipitates were filtered by Whatman filter paper and washed with a 1N HCl solution and distilled water to obtain neutral pH, finally the filtrate was dried at 65 ^{0}C temperature for 24 h to obtain RGO.

The composites of RGO-SnO_2 were prepared by wet mixing method, desired weight percent (wt%) of RGO and desired wt% of SnO_2 were mixed with 20 ml ethanol as the weight ratios of RGO:SnO_2 are (a) 05:95, (b) 10:90, (c) 15:85 and (d) 20:80, were weighed and transferred to a beaker, the solution was homogeneously stirred by magnetic stirrer to get uniform gel like sample. The sample is further heated with hot air oven at 60 ^{0}C for 12 hours and later the prepared sample were ground in an agate mortar and pestle and sent them for further characterizations.

2.3 Characterization Techniques

The prepared samples were subjected to structural, morphological and optical characterizations *viz.*, Xray diffraction (XRD) spectra from Rigaku Smart-lab Cu-K_a radiation wavelength of 1.54 Å, Fourier transform infrared (FTIR) spectra was recorded by Bruker-alpha using KBr pellets, Field Emission Scanning Electron Microscopy (FESEM) images were taken using Zeiss Ultra-55 microscope, High Resolution Electrical results were carried out using waynker Impedance analyzer, gas sensing studies were analyzed by in-house fabricated gas sensing chamber[16,17].

3.0 Results and Discussion

The X-ray diffraction analysis were carried out for the prepared, RGO, SnO_2, RGO:SnO_2 composites which is depicted in the Figure 1, pure single phase SnO_2 nanoparticles were depicted a good crystalline character according to the standard JCPDS file number 41-1445.[18] XRD pattern of RGO showed the broad peak is observed due to the Reduction of oxygen at 25.52^0 & 2θ value of 43.132^0 which confirms the formation of reduced graphene oxide. From the XRD spectra one can confirm the formation of RGO-SnO_2 composites and there are no

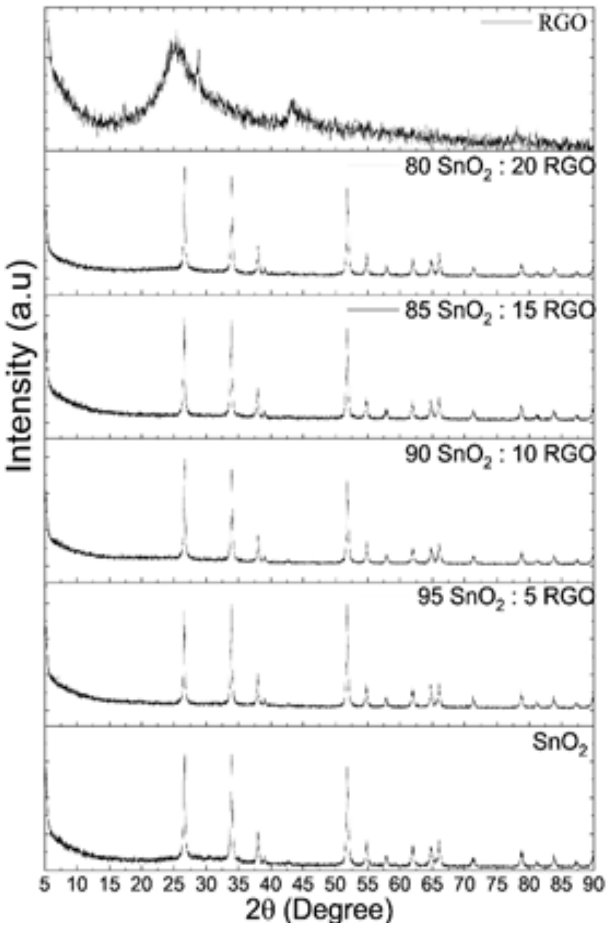

Figure 1. XRD patterns of RGO, SnO_2 and RGO:SnO_2 samples.

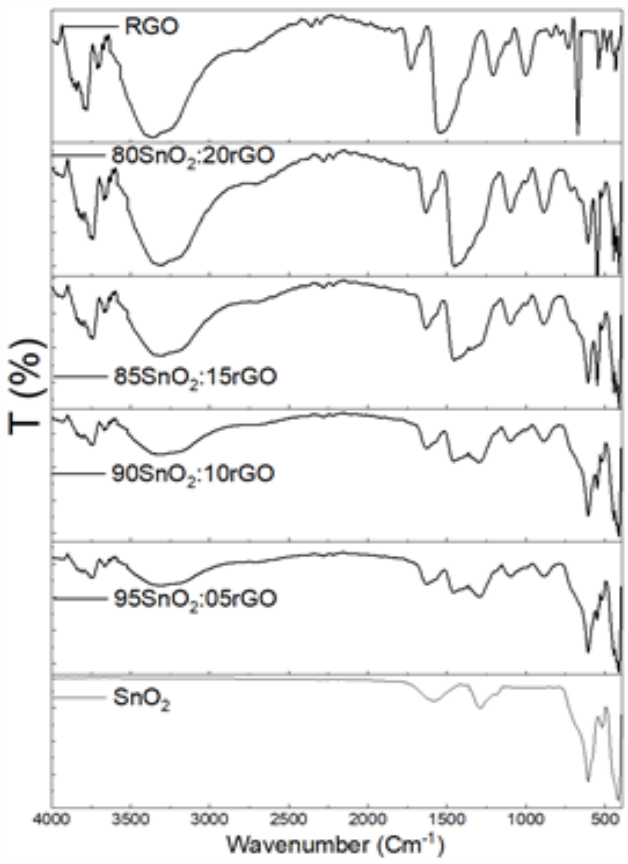

Figure 2. FTIR spectra of RGO, SnO_2 and RGO:SnO_2 samples.

additional peaks were observed from the impurities thus confirms the purity of the sample.

The FTIR spectra of RGO, SnO_2, RGO:SnO_2 composites were depicted in Figure 2. Due to the Reduction of Graphene Oxide some of the functional groups which are present in the Graphene Oxide disappears, we can see these using the FTIR spectroscopy. The typical peaks at 417 & 608 cm^{-1} reveal the presence of the vibration mode of Sn-O from SnO_2, which is more obvious in the RGS composites with increasing the amount of RGO. The band at 1635 cm^{-1} is assigned to the vibration of the adsorbed water molecules as well as to the contributions from the skeletal vibrations of un-oxidized graphitic domains, which are also present in the RGS composites thus confirms the formation of composites. The bands at 1730 and 1060 cm^{-1} are assigned to the C = O and C-OH stretching vibrations of COOH groups which confirm the existance of RGO in the RGS composites. The broad band ranging from 3600 to 3000 cm^{-1} corresponds to the O-H stretching vibrations of adsorbed water molecules.

Figure 3 depicts the FESEM images of RGO, SnO_2, RGO:SnO_2 composites of powdered samples, used to analyze the surface morphology. FESEM images of the SnO_2 particles was found that crystallites of powdered sample are spherical in shape with agglomerated and porous in nature. The SnO_2 sample showing porosity due to the rapid release of large volume of gaseous by-products during the combustion reaction which helps to enhance the adsorption of ethanol molecules on sensor material. Pure RGO sample showing wrinkled in structure due to the reduction RGO from GO, this is due to escape of oxygen atoms which is present on the surface of the GO. The RGS composites shows the SnO_2 particles were decorated on the surface of the RGO sheets as increase in the amount of RGO the SnO_2 particles were uniformly arranged on the surface. Plenty of voids present in the RGS composites benefits the effective contact for the effective charge transfer as a chemiresistive material.

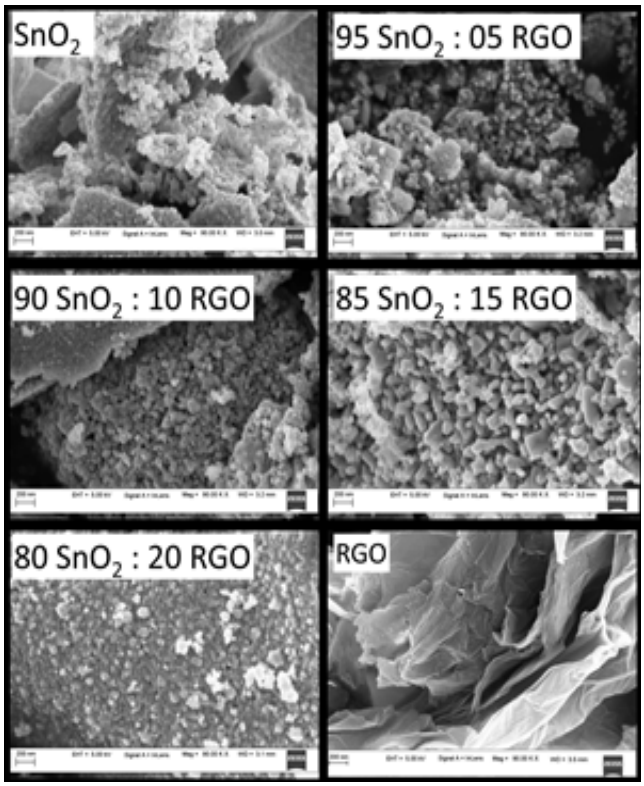

Figure 3. FESEM images of the RGO, SnO_2 and RGO:SnO_2 composite samples.

The complex relative permittivity can be defined as

$$\varepsilon^* = \varepsilon' - j\varepsilon'' \quad (1)$$

ε' & ε" is calculated by the following equations;

$$\varepsilon' = \frac{C}{C_0} = \frac{tC}{A\varepsilon_0} \quad (2)$$

$$\varepsilon'' = \varepsilon' \tan\delta \quad (3)$$

Where, "C" is the capacitance, "t" is the thickness "A" is the area of active electrode surface of the sample holder (cm^2), C_0 is defined as $C_0 = A\varepsilon_0/t$, is the permittivity in free space.

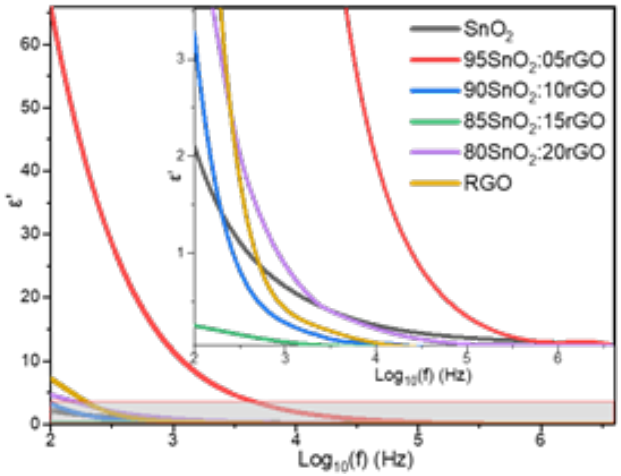

Figure 4. Dielectric constant of the RGO, SnO_2 and RGO:SnO_2 composite samples.

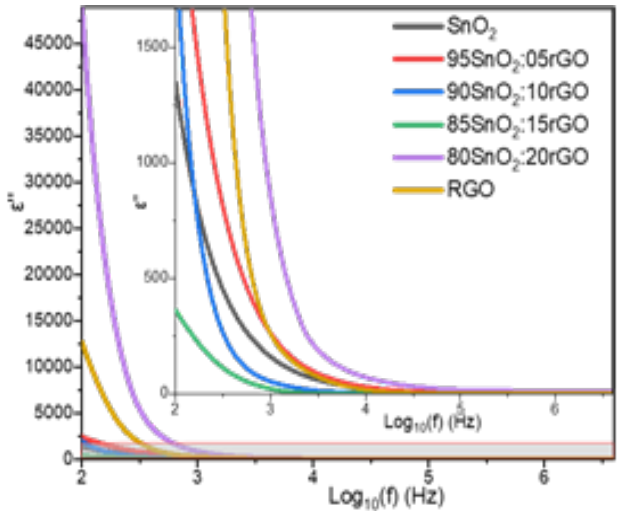

Figure 5. Dielectric loss of the RGO, SnO_2 and RGO:SnO_2 composite samples.

Figure 4 depicts dielectric constant as function of frequency for RGO, SnO_2, RGO:SnO_2 composites of pellet samples. It was observed that as frequency increases the dielectric constant decreases and saturates at higher frequency region this may be attributed due to the Debye-like relaxation mechanism[19]. Compared to all samples 95SnO_2:05RGO composite sample shows high dielectric constant and 85SnO_2:15RGO sample shows low dielectric constant. It was observed that the dielectric loss values decrease with increased frequency and reach constant values at higher frequencies as shown in Figure 5, this happens due to the effect of interfacial polarization in the prepared samples, generally consisting of well-conducting grains separated by poorly conducting grain boundaries, thus revealing dielectric dispersion follows the Maxwell–Wanger double-layer model. This was due to the structural inhomogeneity of the materials.

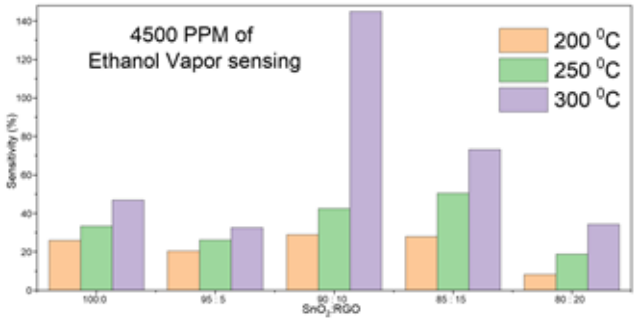

Figure 6. Gas sensing properties of RGO:SnO_2 composite for 4500PPM of ethanol vapors.

Gas sensing measurement were carried out by making use of an in-house fabricated gas sensing chamber. To evaluate the gas sensing response of synthesized RGO, SnO_2 and RGO:SnO_2 composite were deposited as a thick film on an alumina substrate, the conductive silver paste was painted at the two opposite sides of the films to get the ohmic contacts Figure 6. The prepared pellet sample was kept inside the in-house fabricated gas-sensing chamber and the electrical resistance of the sample was measured in normal atmosphere (R_a) and the presence of test gas (R_g) by making use of a multimeter at room temperature[20].

The ethanol vapor sensing studies were characterized for all the prepared samples at 200, 250, 300 ^{0}C temperature are shown in Figure 4. The change in resistance of the sample in the presence and absence of higher PPM of ethanol vapors can be used as the sensing performance

in terms of sensitivity, the sensitivity of the sensor can be calculated by using following equation

Sensitivity (S) % = {(Rg ~ Ra) / Ra } * 100 (4)

The effect of different wt% SnO_2 and RGO incorporated were investigated. The sensing performances of 4500PPM ethanol vapors for all the prepared samples were studied at a 200, 250, and 300^{0}C temperatures which is depicted in the Figure 4. The sensitivities SnO_2 particles for the 4500 PPM of ethanol vapors at 200, 250, and 300^{0}C temperatures was 26, 33, 47% the response time is 33, 26, 24s and the recovered in 133, 162, 189s. For the 4500 PPM of ethanol vapors at 200, 250, and 300 ^{0}C temperatures sensitivities 95SnO_2:05RGO composites was 20, 26, 33% the response time is 46, 23, 18s and the recovery time is 148, 112, 103s. For the 4500 PPM of ethanol vapors at 200, 250, and 300 ^{0}C temperatures sensitivities 90SnO_2:10RGO composites was 29, 42, 145% the response time is 12, 15, 26s and the recovery time is 113, 194, 213s. For the 4500 PPM of ethanol vapors at 200, 250, and 300^{0}C temperatures sensitivities 85SnO_2:15RGO composites was 28, 50, 73% the response time is 9, 26, 33s and the recovery time is 67, 68, 164s. For the 4500 PPM of ethanol vapors at 200, 250, and 300^{0}C temperatures sensitivities 80SnO_2:20RGO composites was 8, 19, 34% the response time is 5, 6, 7s and the recovery time is 134, 173, 223s. From all the composite samples 90SnO_2:10RGO composite sample shows highest sensitivity of 145% which is a good ethanol sensor material.

4.0 Conclusions

The SnO_2, RGO and RGO-SnO_2 composite were successfully prepared, the prepared samples confirmed the formation by XRD and FTIR spectroscopy. The SnO_2 particles show spherical in shape with agglomerated and porous in nature, increase in addition percentage of RGO prevent agglomeration of SnO_2 particles, which in turn inhibits restacking of the RGO sheets; the resultant composites show porous high specific surface area nanohybrid with enhanced oxygen adsorption capabilities and suitable ethanol sensing features. The dielectric constant and dielectric loss spectra of prepared samples shows similar behavior as that of frequency increases there is a decrease in both spectra this is occurs due to the effect of interfacial polarization in the materials. The ethanol vapor sensing studies were conducted at 3 different temperatures of 200, 250 and 300 ^{0}C using in-house fabricated gas sensing chamber, compared to all the samples 90SnO_2:10RGO composites shows high sensitivity of 145% for the 4500PPM of ethanol vapors with the response time of 26s and recovered in 213s. Thus synthesized RGS samples are having good stoichiometric compositions and excellent quality which justifies the method of synthesis varies the properties of the sample and percentage of dopants leads to enhance the properties of the material.

5.0 Acknowledgement

The authors Kiranakumar H V, Naveen C S and Thejas R are thankful to Presidency University, Bengaluru for the financial support and for providing laboratory facilities.

6.0 Declaration of Interest

The authors declare that they have no known competing financial interests or personal relationships that could have appeared to influence the work reported in this paper.

7.0 References

1. Dai ZR, Gole JL, Stout JD, Wang ZL. Tin Oxide Nanowires, Nanoribbons, and Nanotubes. J Phys Chem B. 2002 Feb 1; 106(6):1274–9.
2. Hyodo T, Abe S, Shimizu Y, Egashira M. Gas-sensing properties of ordered mesoporous SnO2 and effects of coatings thereof. Sens Actuators B Chem. 2003 Aug 1; 93(1):590–600.
3. Li M, Qiao LJ, Chu WY, Volinsky AA. Water pre-adsorption effect on room temperature SnO2 nanobelt ethanol sensitivity in oxygen-deficient conditions. Sens Actuators B Chem. 2011 Nov 15; 158(1):340–4.
4. Comini E, Faglia G, Sberveglieri G, Calestani D, Zanotti L, Zha M. Tin oxide nanobelts electrical and sensing properties. Sens Actuators B Chem. 2005 Nov 11; 111–112:2–6.
5. Rajeeva MP, Jayanna HS, Naveen CS, Lamani A. Size Controlled Effect of Oxidizer in Synthesis of Tin (IV) Oxide Nanomaterial by Gel Combustion Method. In: Proceedings of National Conference On Recent Trends in Physics,Mathematics and Engineering. Mysore; 2015. p. 6.

6. Kiranakumar. H. V, Thejas R, Naveen C S, Khan MI, Prasanna G D, Reddy S, et al. A review on electrical and gas-sensing properties of reduced graphene oxide-metal oxide nanocomposites. Biomass Convers Biorefinery [Internet]. 2022 Sep 3; Available from: https://doi.org/10.1007/s13399-022-03258-7
7. Compton OC, Nguyen ST. Graphene Oxide, Highly Reduced Graphene Oxide, and Graphene: Versatile Building Blocks for Carbon-Based Materials. Small. 2010 Mar 22; 6(6):711–23.
8. Bârsan N, Ionescu R. The mechanism of the interaction between CO and an SnO2 surface: the role of water vapour. Sens Actuators B Chem. 1993 Mar 15; 12(1):71–5.
9. Su PG, Zheng YX. A room temperature NH3 gas sensor based on a quartz crystal microbalance coated with a rGO–SnO2 composite film. Anal Methods. 2022 Apr 7; 14(14):1454–61.
10. Comini E, Faglia G, Sberveglieri G, Pan Z, Wang ZL. Stable and highly sensitive gas sensors based on semiconducting oxide nanobelts. Appl Phys Lett. 2002 Sep 2; 81(10):1869–71.
11. Charishma, Jayarama A, Shastrimath VD, Pinto R, Adyanthaya NM. An Ethanol Sensor Review : Materials , Techniques and Performance. Sahyadri Int J Res. 2017; 3(1):37–46.
12. Rajeeva MP, Naveen CS, Lamani AR, Jayanna HS. Synthesis, Characterization and Electrical Conductivity of High Porous Tin Oxide Nanocrystallites for Ethanol Sensing. Mater Today Proc. 2017 Jan 1; 4(11, Part 3):12094–102.
13. Zaaba NI, Foo KL, Hashim U, Tan SJ, Liu WW, Voon CH. Synthesis of Graphene Oxide using Modified Hummers Method: Solvent Influence. Procedia Eng. 2017 Jan 1; 184:469–77.
14. Shahriary L, Athawale AA. Graphene oxide synthesized by using modified hummers approach. Int J Renew Energy Environ Eng. 2014 Jan; 2(1).
15. Sharma N, Sharma V, Jain Y, Kumari M, Gupta R, Sharma SK, et al. Synthesis and Characterization of Graphene Oxide (GO) and Reduced Graphene Oxide (rGO) for Gas Sensing Application. Macromol Symp. 2017; 376(1):1700006.
16. Umapathy G, Senguttuvan G, John Berchmans L, Sivakumar V. Structural, dielectric and AC conductivity studies of Zn substituted nickel ferrites prepared by combustion technique. J Mater Sci Mater Electron. 2016 Jul 1; 27(7):7062–72.
17. Thejas R, Soundarya TL, Nagaraju G, Swaroop K, Prashantha SC, Veena M, et al. Effect of cation concentration on structural, morphology, optical properties of Zinc-Nickel ferrite nanoparticles. Mater Lett X. 2022 Sep 1; 15:100156.
18. Rajeeva MP, Naveen CS, Lamani AR, Jayanna HS. Size and frequency dependent dielectric properties of tin (IV) oxide nanoparticles synthesized by gel combustion method. AIP Conf Proc. 2013 Jun 3; 1536(1):183–4.
19. Sakellis I, Papathanassiou AN, Grammatikakis J. Effect of composition on the dielectric relaxation of zeolite-conducting polyaniline blends. J Appl Phys. 2009 Mar 15; 105(6):064109.
20. Thejas R, Prasanna G, Nagaraju G, Murugendrappa M, Naveen C. Enhanced gas-sensing performance at room temperature and electrical properties of polyaniline–$Ni_{0.6}Zn_{0.4}Fe_2O_4$ nanocomposites. Proc Inst Mech Eng Part E J Process Mech Eng. 2022 May 16; 09544089221100778.